



HAL
open science

Temperature estimation in fusion devices using machine learning techniques on infrared specular synthetic data

Alexis Juven, Marie-Helene Aumeunier, Romain Brunet, Mickael Le Bohec, Mouloud Adel, Roberto Miorelli, Xavier Artusi, Christophe Reboud

► To cite this version:

Alexis Juven, Marie-Helene Aumeunier, Romain Brunet, Mickael Le Bohec, Mouloud Adel, et al.. Temperature estimation in fusion devices using machine learning techniques on infrared specular synthetic data. IVMSP 2022 - IEEE 14th Image, Video, and Multidimensional Signal Processing Workshop, Jun 2022, Nafplio, Greece. 10.1109/IVMSP54334.2022.9816270 . cea-04555865

HAL Id: cea-04555865

<https://cea.hal.science/cea-04555865>

Submitted on 23 Apr 2024

HAL is a multi-disciplinary open access archive for the deposit and dissemination of scientific research documents, whether they are published or not. The documents may come from teaching and research institutions in France or abroad, or from public or private research centers.

L'archive ouverte pluridisciplinaire **HAL**, est destinée au dépôt et à la diffusion de documents scientifiques de niveau recherche, publiés ou non, émanant des établissements d'enseignement et de recherche français ou étrangers, des laboratoires publics ou privés.

Temperature Estimation in Fusion Devices using Machine Learning techniques on Infrared Specular Synthetic Data

Alexis Juven, Marie-Hélène Aumeunier
Romain Brunet, Mickaël Le Bohec
CEA, IRFM
Saint-Paul-lez-Durance, Cadarache, France

Mouloud Adel
CNRS, Aix-Marseille Université
Centrale Marseille, Institut Fresnel
UMR 7249 13013 Marseille, France

Roberto Miorelli, Xavier Artusi,
Christophe Reboud
Université Paris-Saclay, CEA, List
F-91120, Palaiseau, France

Abstract—Infrared (IR) imaging systems are common diagnostics for monitoring in-vessel components in thermonuclear fusion devices (tokamak). Nevertheless, IR interpretation in fully metallic environment is complex due to the presence of multiple reflections and the change of optical properties of materials as the fusion operation progresses. This causes high errors on the surface temperature measurement which is a risk for machine protection. The paper presents a first demonstration of simulation-assisted machine learning method for retrieving the surface temperature from IR measurement on metallic targets with unknown properties. The technique relies on the training of a convolutional neural network on a synthetic dataset generated by a deterministic ray tracer. The performances of such an approach is first proven on tokamak prototype considering pure specular surfaces.

I. INTRODUCTION

Infrared (IR) thermography system are key diagnostics to monitor the surface temperature of plasma-facing components in fusion devices (tokamak). Such systems is widely used in existing fusion devices (WEST [1], ASDEX-Upgrade [2], JET [3]). In the future international fusion devices ITER, under construction at Cadarache (France), a wide network of 21 visible and IR cameras is planned to monitor almost the whole chamber (800 m^2) on a wide temperature range between 200 and 3600 °C [4], [5]. Nevertheless the interpretation of IR measurement is not straightforward. Indeed, the tokamak chamber is composed of metallic materials characterized by low and variable emissivity. As a consequence, the collected flux by the camera includes both an emission part, coming directly from the target to be monitored, but also a reflective part coming from the multiple reflections in the chamber. In addition the emission part, related to the target temperature (following to the Planck's law), is weighted by an emissivity factor of target that can change during the machine exploitation regime. These cause high errors on the surface temperature [6] which is a risk for machine protection and the smooth progress of plasma operations. A bad estimation of the reflections can lead to misinterpretations between a hot spot and a reflection of a hot spot on a cold surface, which would potentially trigger a false alarm and an unnecessary stop of the machine. Poor emissivity estimation could lead to an underestimation of the component temperature, potentially damaging the machine.

In this paper, we propose a numerical approach aiming at estimating temperatures and emissivities in fully metallic and

radiative environments. Similar problematic is addressed by the inverse rendering community. In this case, it is a matter of deducing information on the observed scene in the visible from photos: either to reconstruct the geometry of scene or to estimate lighting or to estimate the materials properties. Many of recent work are based on machine learning (ML) techniques using synthetic data to train inverse model for indoor scene [7]–[9]. But applications for estimating temperature from thermal scene remains marginal to the best of our knowledge.

This paper presents a first demonstration of temperature estimation in fusion devices using machine learning techniques trained on simulated data set. The first section focuses on the development of deterministic ray tracer able to simulate quickly infrared images from pure specular thermal scene. The second and third sections describe the generation of optimal synthetic library and the implementation of ML algorithms. In the last section, the first results on temperature and emissivity estimation and next developments are discussed.

II. DIRECT MODEL BY SPECULAR RAY TRACING

A. Overview of existing direct models

Two direct radiative models are currently used to simulate IR images in fusion devices. A first one is based on Monte Carlo Ray Tracing code able to propagate the rays in 3D complex geometry by taking into account complex thermo-radiative and optical properties of materials. Such a model uses the Bidirectional Distribution Reflectivity Function (BRDF) to describe the angular and spectral dependance of materials reflectance. The angular dependance of target emission is also considered. The detailed simulations are usually used to help IR interpretation (in a qualitative way) in current fusion devices as WEST and ASDEX-Upgrade [10] and to predict IR behavior in future devices as ITER (the biggest international machine under construction) [6]. Nevertheless, such a code requires high computing time (typically 12 hours on a 4-core CPU), which strongly limits the amount of data that can be generated and the possibility to create a wide dataset. A second analytical model based on radiosity methods has been so developed to generate an IR image in a few seconds [11]. But such a model assumes diffuse surface, meaning that the reflected and emitted flux is equal for all incident and viewing direction. This strong assumption of diffuse surface is not quite relevant for materials in fusion devices, that

seems to have a strong specular component. We present a new fast radiative model, named *Speculos*, assuming pure specular surface, developed in order to train machine learning model from a large simulated dataset.

B. *Speculos*

Speculos is a "deterministic" ray tracer able to propagate rays in 3D meshed geometry assuming pure specular surface. The image is generated by backward ray tracing: a ray defined by a starting point and a direction \mathbf{u} is launched through a pinhole camera. The intersection of rays with geometry of 3D thermal scene is computed using Intel Embree tool [12], which implements a parallel CPU intersection primitive using Bounded Volume Hierarchies [13]. At each intersection, a new direction $\mathbf{u}_{\text{reflected}}$ is computed following to the Snell-law Descartes as described in Eq. 1. The ray path is so computed recursively:

$$\mathbf{u}_{\text{reflected}} = \mathbf{u} - 2 \langle \mathbf{u}, \mathbf{n} \rangle \mathbf{n} \quad (1)$$

where $\mathbf{u}_{\text{reflected}}$ is the direction vector of reflected rays, \mathbf{u} is the direction vector of incident rays, \mathbf{n} the intersected face normal computed from with Phong interpolation using the barycentric coordinates of the intersection point [14], and $\langle \cdot, \cdot \rangle$ the scalar product.

Once rays path calculation is done, the leaving luminance at each intersected face is computed following to the light transport equation Eq. 2 assuming specular surface [15]:

$$L_i = \varepsilon_i L^\circ(T_i) + (1 - \varepsilon_i) L_{i+1} \quad (2)$$

where L_i is the leaving luminance at the intersection i , ε_i the emissivity of the intersected face, $L^\circ(T_i)$ the emitted flux computed from Planck's law (in $W.m^{-2}.sr^{-1}$) using the face temperature T_i , and L_{i+1} (in $W.m^{-2}.sr^{-1}$) the incident flux coming from the next intersected face.

For each ray, the list of temperatures and emissivities ($T_0, \varepsilon_0, T_1, \varepsilon_1, \dots$) of the different intersected faces is saved and the total flux collected by camera pixel is computed. Last, the final luminance on each camera pixel is provided by averaging the luminance computed from 16 rays launched from evenly spaced positions within the pixel. This allows to be more precise in case of low resolution imaging system and non uniform thermal scene.

The ray intersection algorithm is performed by the CPU on several threads, which requires a computational time of several seconds to tens of seconds. However, once the pure geometric computation of the ray paths is done, it can be used to generate as many images as desired by varying only the properties of the surfaces but not the camera view. Ray luminance computations are parallelized on the GPU using CUDA kernels [16], which allows to generate a large number of images in a reasonable time (around one to five images per second). This makes *Speculos* suitable for the creation of large datasets covering a wide range of surface property scenarios.

III. GENERATION OF SYNTHETIC LIBRARY

A. Thermal scene modeling

Figure 1 shows the scene observed from a tangential wide angle view of WEST tokamak. The 3D model is split

into 36 components. Each component is assigned an uniform temperature and emissivity except for divertor. The divertor is a key component receiving the maximum heat load (up to $10 MW.m^{-2}$ in steady state) and presents a peaked temperature profile, roughly modelled from Eich equation in [17]. Such a thermal scene is described with 75 parameters (36 emissivities by components, 35 temperatures on components with uniform temperature and 4 parameters to define the temperature distribution on divertor). A pinhole camera model is used to reproduce the experimental IR image (640×512 pixels of $15 \mu m$ in the filter band $3900-4100 nm$). An example of generated picture can be seen in figure 2 next to an example of an image captured during experiments.

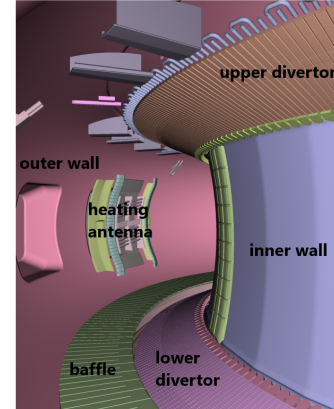


Fig. 1: 3D model of the tokamak seen from the camera point of view, using a different color per component. Each component is characterized by an uniform temperature and uniform emissivity, except for the lower divertor for which heat flux model (based on Eich equation) is applied.

B. Generation of random scenes

A first database of 15000 images has been performed from ray tracing *Speculos* by changing input parameters of models (75 parameters). The scenario covered by this simulated database are based on WEST tokamak experiences: the temperature of first wall is between $90^\circ C$ and $110^\circ C$, the temperature of the closest in-vessel components (e.g bumper, antenna outboard) is assumed to be varied between $300^\circ C$ and $500^\circ C$. The maximum temperature of divertor temperature profile can rise to $1800^\circ C$. The materials emissivity range is fixed further to experimental measurements: between 0.05 and 0.5. Last, latin hypercube sampling is used to cover optimally the parameters range [18].

The database used for training machine learning is composed of triplet of images:

- the simulated camera image in apparent temperature, which is the equivalent blackbody temperature (assuming emissivity equal to 1). This image is deduced from luminance image (in $W.m^{-2}.sr^{-1}$) computed from *Speculos* ray tracing and by inverting Planck's law;
- the true temperature image, giving the true surface temperature for each pixel of camera;

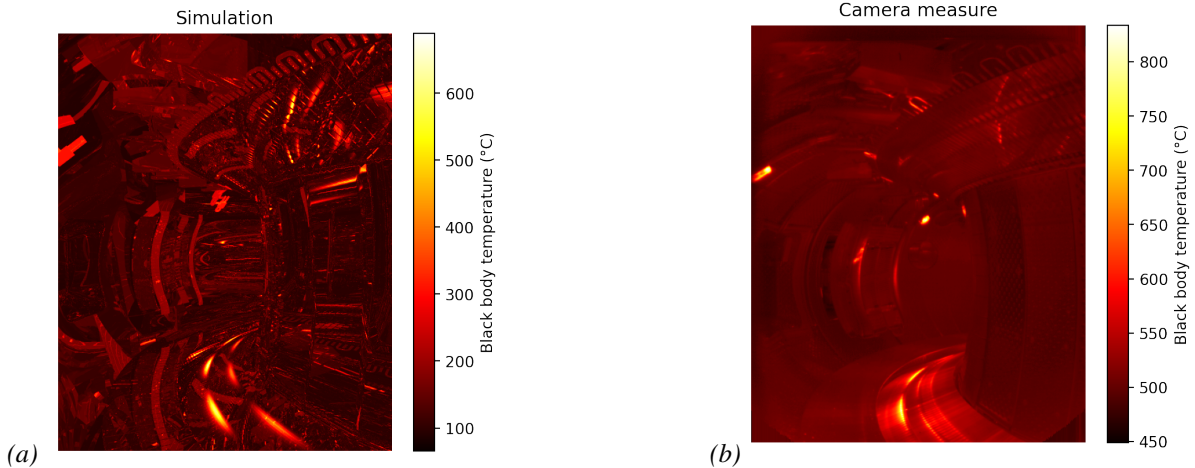


Fig. 2: (a) Simulated infrared images from *Speculos* (assuming pure specular reflections). (b) Experimental image from WEST wide-angle camera for qualitative comparison with simulation. The parameters used for the simulation do not correspond to the experimental image, hence the different luminosities. For both images, a reflection of the lower divertor pattern can be observed on the upper divertor.

- the true emissivity image, giving the target emissivity for each pixel.

The true temperature and emissivity images are deduced from the 3D thermal scene used as input of ray tracing code through an operation of 3D to 2D projection. After converting 3D points of thermal scene into 2D points on the camera view plane, the true temperature (or emissivity) is deduced for each pixel by averaging the associated temperature (or emissivity) of 3D points.

IV. MACHINE LEARNING FOR MODEL INVERSION

Supervised machine learning is performed from a simulated dataset in order to propose an inverse algorithm that deduces the temperature and emissivity map of visible surfaces from a thermal scene image.

A. Architecture

We implemented a deep fully convolutional neural network, inspired from the original U-Net architecture from [19]. Such a network allows to learn "image to image" functions and it is particularly adapted in our case where the output images (temperature or emissivity maps) contain similar details and object localization as the input one (apparent temperature map). The architecture of implemented network is described in Figure 3. The image sizes are adapted to those of the infrared camera: 512 pixels wide by 640 high, and the number of pooling operations is increased (6 instead of 4 in the original model) in order to propagate a global information to every output pixel, which is essential when dealing with the non local property of reflections. To fit memory limitations, the initial number of convolution channel is reduced (32 instead of 64). Since the network is used for a regression task, no activation function is used for the output layer.

B. Learning process

The network receives in input a single channel image (apparent black body temperature map) and returns a two channel image (temperature and emissivity maps of visible surfaces). These images are normalized: temperature and emissivities are mapped into the interval $[0; 1]$ using the minimum and maximum encountered values in the training set. Input images are standardized using the mean value and standard deviation on the training set.

The dataset of 15000 scenes was split into a training set of 10000 elements, a validation set of 2000 elements and a testing set of 3000 elements. The training was performed using the adam optimizer on the mean squared error loss during 100 epochs, about 16 hours of training time on a NVIDIA Tesla V100 PCIe 32 GB GPU. In order to fit the card memory limitations, batches of size 10 were used, and randomly shuffled after each epoch. The network with the lowest error rate on the validation set is used to evaluate its performances on the testing set.

C. Results on synthetic data for specular reflections

After learning, the network is evaluated on the test dataset of 3000 images. We are interested in the mean temperature error computed from the 3000 test images on each main in-vessel component. The mean temperature error for in-vessel components with uniform temperature (baffle, wall, bumper, etc) is 4.8 °C (4.3% mean relative error), which is a good improvement compared to usual method causing an error of 41°C by assuming blackbody (i.e. assuming emissivity of 1 for all targets and no reflection).

Figure 4 shows the temperature error for the divertor characterized by non-uniform temperature. The mean relative error is shown for different real temperature range. Indeed the lower temperature will more sensitive to reflections whereas the higher temperature will sensitive to emissivity inaccuracy. The temperature error are more important for lower temperature (<200°C) even if they are quite in the ITER specification

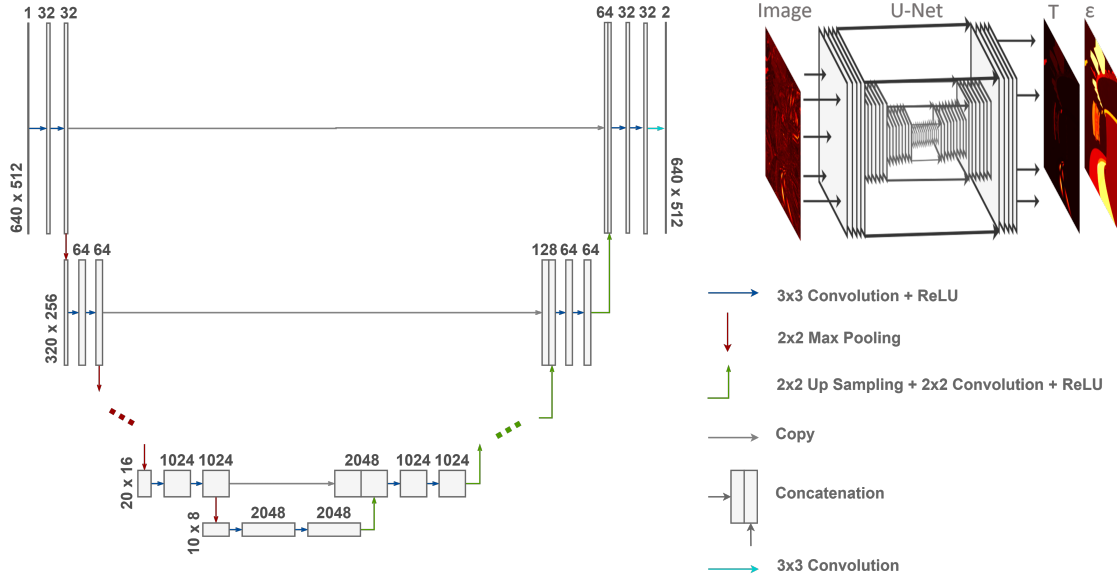


Fig. 3: Neural network architecture implemented to return temperature and emissivity maps from infrared camera measures, with slight changes from the original published U-Net architecture [19].

(20% error required for lower temperature below 400 °C and 10% error for higher temperature). The higher temperature are very well estimated with an error better than 1.5%, which suggest that emissivity should be also quite evaluated by algorithms. This is confirmed by figure 5, that shows the absolute emissivity error as a function of real target emissivity: the emissivity value is estimated with a precision better than 0.05.

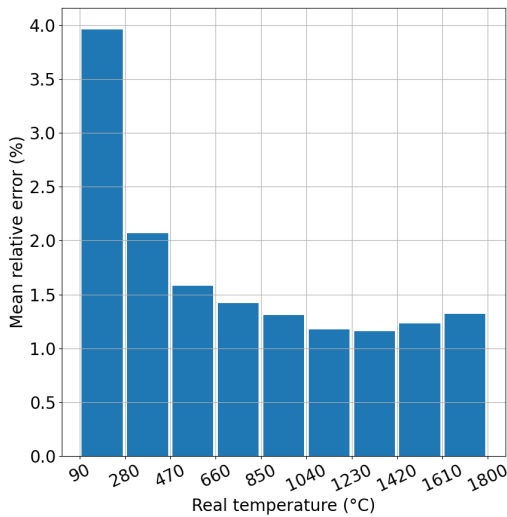


Fig. 4: Testing set mean relative error (%) on divertor temperature estimation per temperature range.

V. DISCUSSION AND CONCLUSIONS

We have presented a first method based on supervised deep learning trained on synthetic database to estimate simultane-

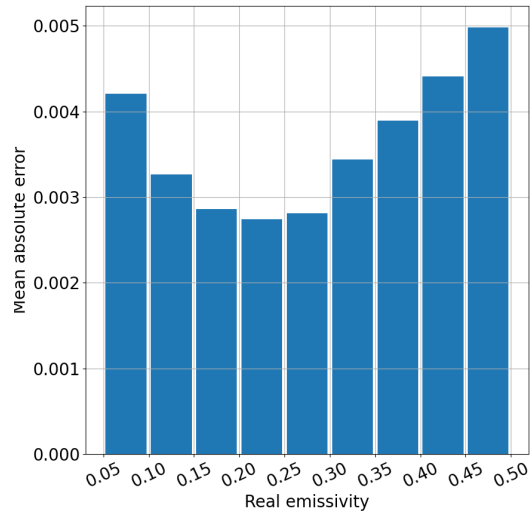


Fig. 5: Testing set mean absolute error on divertor emissivity estimation per emissivity range.

ously the temperature and emissivity from infrared images. We have shown that temperature and emissivity can be estimated with high accuracy (respectively better than 5% and 0.05) under the assumptions of pure specular reflections.

There are many extensions to be considered for future works. First, we have to extend the possible scenarios range by considering more complex temperature and emissivity distributions more relevant to tokamak experience. Non-lambertian emission will be also implemented. Successively, more realistic models of reflectivity including diffuse part and a specular part (e.g. following to a gaussian distribution around the Snell-

Descartes laws) will be considered. Toward this end, stochastic Monte Carlo algorithms are envisaged. In order to mitigate the computational burden entailed by Monte Carlo simulations, several solutions may be investigated at this stage. From the numerical simulation point of view, hardware acceleration based on the full exploitation of GPU-based-calculations of Monte Carlo simulations is under study. From the ML perspective, the use of transfer learning methods and/or generative deep neural network architectures [20]–[22] will be taken into account.

ACKNOWLEDGMENT

This work has been carried out within the framework of the EUROfusion Consortium, funded by the European Union via the Euratom Research and Training Programme (Grant Agreement No 101052200 — EUROfusion). Views and opinions expressed are however those of the author(s) only and do not necessarily reflect those of the European Union or the European Commission. Neither the European Union nor the European Commission can be held responsible for them.

REFERENCES

- [1] X. Courtois, M. Aumeunier, C. Balorin, J. Migozzi, M. Houry, K. Blanckaert, Y. Moudou, C. Pocheau, A. Saille, E. Hugot, M. Marcos, and S. Vives, “Full coverage infrared thermography diagnostic for west machine protection,” *Fusion Engineering and Design*, vol. 146, pp. 2015–2020, 2019, sI:SOFT-30.
- [2] B. Sieglin, M. Faitsch, A. Herrmann, B. Brucker, T. Eich, L. Kammerloher, and S. Martinov, “Real time capable infrared thermography for asdex upgrade,” *Review of Scientific Instruments*, vol. 86, no. 11, p. 113502, 2015.
- [3] T. Eich, A. Herrmann, P. Andrew, and A. Loarte, “Power deposition measurements in deuterium and helium discharges in jet mkiigb divertor by ir-thermography,” *Journal of Nuclear Materials*, vol. 313-316, pp. 919–924, 2003, plasma-Surface Interactions in Controlled Fusion Devices 15. [Online]. Available: <https://www.sciencedirect.com/science/article/pii/S0022311502014770>
- [4] R. Reichle, E. de la Cal, Y. Corre, M. Joanny, A. Manzanares, J. L. de Pablos, S. Salasca, and J.-M. Travere, “On the operational specifications and associated ramp;d for the vis/ir diagnostic for iter,” in *2009 1st International Conference on Advancements in Nuclear Instrumentation, Measurement Methods and their Applications*, 2009, pp. 1–7.
- [5] L. Letellier, C. Guillon, M. Ferlet, M.-H. Aumeunier, T. Loarer, E. Gauthier, S. Balme, B. Cantone, E. Delchambre, D. Elbèze, S. Larroque, F. Labassé, D. Blanchet, Y. Penelieu, L. Rios, F. Mota, C. Hidalgo, A. Manzanares, V. Martin, F. L. Guern, R. Reichle, and M. Kocan, “System level design of the iter equatorial visible/infrared wide angle viewing system,” *Fusion Engineering and Design*, vol. 123, pp. 650–653, 2017, proceedings of the 29th Symposium on Fusion Technology (SOFT-29) Prague, Czech Republic, September 5-9, 2016.
- [6] M.-H. Aumeunier, M. Kočan, R. Reichle, and E. Gauthier, “Impact of reflections on the divertor and first wall temperature measurements from the iter infrared imaging system,” *Nuclear Materials and Energy*, vol. 12, pp. 1265–1269, 2017.
- [7] Y. Yu and W. A. P. Smith, “Inverserendernet: Learning single image inverse rendering,” in *Proceedings of the IEEE/CVF Conference on Computer Vision and Pattern Recognition (CVPR)*, June 2019.
- [8] S. Sengupta, J. Gu, K. Kim, G. Liu, D. W. Jacobs, and J. Kautz, “Neural inverse rendering of an indoor scene from a single image,” in *Proceedings of the IEEE/CVF International Conference on Computer Vision (ICCV)*, October 2019.
- [9] Z. Li, M. Shafiei, R. Ramamoorthi, K. Sunkavalli, and M. Chandraker, “Inverse rendering for complex indoor scenes: Shape, spatially-varying lighting and svbrdf from a single image,” in *Proceedings of the IEEE/CVF Conference on Computer Vision and Pattern Recognition (CVPR)*, June 2020.
- [10] M.-H. Aumeunier, J. Gerardin, C. Talatizi, M. Le Bohec, M. Ben Yaala, L. Marot, T. Loarer, R. Mitteau, J. Gaspar, F. Rigollet, X. Courtois, M. Houry, A. Herrmann, and M. Faitsch, “Infrared thermography in metallic environments of west and asdex upgrade,” *Nuclear Materials and Energy*, vol. 26, p. 100879, 2021. [Online]. Available: <https://www.sciencedirect.com/science/article/pii/S2352179120301447>
- [11] C. Talatizi, M.-H. Aumeunier, F. Rigollet, M. L. Bohec, C. L. Niliot, and A. Herrmann, “Solving the infrared reflections contribution by inversion of synthetic diagnostics: First results on west,” *Fusion Engineering and Design*, vol. 171, p. 112570, 2021. [Online]. Available: <https://www.sciencedirect.com/science/article/pii/S092037962100346X>
- [12] I. Wald, S. Woop, C. Benthin, G. S. Johnson, and M. Ernst, “Embree: A kernel framework for efficient cpu ray tracing,” *ACM Trans. Graph.*, vol. 33, no. 4, jul 2014. [Online]. Available: <https://doi.org/10.1145/2601097.2601199>
- [13] J. Klosowski, M. Held, J. Mitchell, H. Sowizral, and K. Zikan, “Efficient collision detection using bounding volume hierarchies of k-dops,” *IEEE Transactions on Visualization and Computer Graphics*, vol. 4, no. 1, pp. 21–36, 1998.
- [14] B. T. Phong, “Illumination for computer generated pictures,” *Commun. ACM*, vol. 18, no. 6, p. 311–317, jun 1975. [Online]. Available: <https://doi.org/10.1145/360825.360839>
- [15] J. T. Kajiya, “The rendering equation,” *SIGGRAPH Comput. Graph.*, vol. 20, no. 4, p. 143–150, aug 1986. [Online]. Available: <https://doi.org/10.1145/15886.15902>
- [16] J. Nickolls, I. Buck, M. Garland, and K. Skadron, “Scalable parallel programming with cuda: Is cuda the parallel programming model that application developers have been waiting for?” *Queue*, vol. 6, no. 2, p. 40–53, mar 2008. [Online]. Available: <https://doi.org/10.1145/1365490.1365500>
- [17] T. Eich, B. Sieglin, A. Scarabosio, W. Fundamenski, R. J. Goldston, and A. Herrmann, “Inter-elm power decay length for jet and asdex upgrade: Measurement and comparison with heuristic drift-based model,” *Phys. Rev. Lett.*, vol. 107, p. 215001, Nov 2011. [Online]. Available: <https://link.aps.org/doi/10.1103/PhysRevLett.107.215001>
- [18] M. D. McKay, R. J. Beckman, and W. J. Conover, “A comparison of three methods for selecting values of input variables in the analysis of output from a computer code,” *Technometrics*, vol. 21, no. 2, pp. 239–245, 1979. [Online]. Available: <http://www.jstor.org/stable/1268522>
- [19] O. Ronneberger, P. Fischer, and T. Brox, “U-net: Convolutional networks for biomedical image segmentation,” in *Medical Image Computing and Computer-Assisted Intervention – MICCAI 2015*, N. Navab, J. Hornegger, W. M. Wells, and A. F. Frangi, Eds. Cham: Springer International Publishing, 2015, pp. 234–241.
- [20] A. Antoniou, A. Storkey, and H. Edwards, “Data augmentation generative adversarial networks,” 2017. [Online]. Available: <https://arxiv.org/abs/1711.04340>
- [21] V. Sandfort, K. Yan, P. J. Pickhardt, and R. M. Summers, “Data augmentation using generative adversarial networks (CycleGAN) to improve generalizability in CT segmentation tasks,” vol. 9, no. 1, p. 16884. [Online]. Available: <https://doi.org/10.1038/s41598-019-52737-x>
- [22] R. Brunet, M.-H. Aumeunier, R. Miorelli, C. Reboud, X. Artusi, and M. L. Bohec, “Infrared measurement synthetic database for inverse thermography model based on deep learning,” *32 SYMPOSIUM ON FUSION TECHNOLOGY DUBROVNIK, CROATIA 18-23 SEPTEMBER 2022*.